AIAA SciTech Forum
9 - 13 January 2017, Grapevine, Texas
55th AIAA Aerospace Sciences Meeting

Initial Weight Estimate of Advanced Transport Aircraft Concepts Considering Aeroelastic Effects

Gabriel P. Chiozzotto[1]
German Aerospace Center (DLR), Göttingen, 37073, Germany

This paper presents a semi-empirical method for the weight estimation of advanced transport aircraft concepts in early design stages. The aircraft weight is estimated according to four component groups with different sizing drivers. Emphasis is placed on the wing weight estimation considering aeroelastic effects. A physics-based wing weight estimation tool is used in a Design of Experiments and the results are applied in a least-squares regression obtaining wing Weight Estimating Relationships (WERs). Typical parameters covering a wide design space are considered so the method is applicable to business jets, regional turboprops, short-range and long-range transport aircraft. The WERs equations are presented in typical handbook form for simple application. Static aeroelastic loads, aileron efficiency and aeroelastic divergence effects on the wing weight are considered. Equations are presented for conventional transport aircraft, forward swept wing, strut-braced wing, and forward-swept strut-braced wing concepts. The WERs are applicable to aluminum or carbon-fiber reinforced plastic wings. The equations are verified for accuracy with available designs and the sensitivities are checked against the weights tool used to generate them. Application of the method in a simple design study illustrates its usefulness in quickly assessing different concepts for a set of requirements.

I. Introduction

AIRCRAFT conceptual design usually consists of the following activities: 1) assessment of different aircraft concepts and technologies for a certain mission, 2) evaluation and definition of a realistic set of design requirements, and 3) initial sizing of the aircraft for more detailed analyses in the preliminary design phase. To accomplish these tasks, engineers usually rely on simple handbook methods as presented in many design books[1-4] and design studies[5-7]. The handbook methods are a very useful approach even with the advent of modern computers. They provide fast, flexible and easily understood means for performing design studies. Nevertheless, due to their semi-empirical nature, they are often not considered suitable in assessing advanced concepts. This restriction is mainly caused by the database used in the preparation of the equations and not due to the handbook equations as a methodology.

Weights estimation is particularly important in conceptual design due to the effect on overall performance, size and costs. Typical handbook methods for weights estimation consist of Weight Estimating Relationships (WERs) based on simple physical expressions correlated with historical data on aircraft weights[4,8]. Among the different components whose weights are to be estimated, the wing structure is usually considered in greater detail. This occurs due to the following reasons: 1) the wing weight is usually between 15% and 25% of the aircraft Operating Empty Weight (OEW), 2) the wing weight is very sensitive to changes in the design variables, which are generally directly related to the wing geometry due to its effect on the aircraft performance, and 3) the wing weight growth due to changes in the total aircraft weight is usually very high since the wing is designed to lift most of the aircraft weight in flight. Because of these facts, many detailed wing weight estimation methods of different complexity have been developed for application in early design[9-15]. Nevertheless, these methods are either too complex for early

[1]Research Engineer, Loads Analysis and Design, Institute of Aeroelasticity, Gabriel.PinhoChiozzotto@dlr.de, AIAA Member.

conceptual design studies or are simple but suitable only for conventional configurations without consideration of aeroelastic effects.

When advanced concepts such as the Strut-Braced Wing (SBW) or the Forward Swept Wing (FSW) are considered, or when the designer wants to account for aeroelastic effects when increasing the wing span for example, the classical handbook WERs are not sufficient for design. In these situations, the designer either applies some correction factors to the WERs available or waits until more detailed analyses are available. But until the point that more refined analyses can be performed, the design has already evolved to the point that some decisions about the configuration are already done.

This paper addresses this problem by providing an effective handbook methodology for initial weight estimate in the conceptual design of advanced configurations. The initial weight estimate method proposed by Scott and Nguyen[16] is extended with wing WERs developed for advanced concepts considering aeroelastic effects. The WERs are developed with space filling Design of Experiments (DoE) results from a wing weight estimation tool[11]. This improves the quality of the WERs since: 1) the DoE fills the design space uniformly avoiding bias due to certain inherent characteristics in a purely historical database, and 2) the WERs are based on physical principles as represented in the more detailed wing weight tool.

The paper is organized as follows: in the following sections an overview of previous similar work and definition of the scope of this work is presented. In Section II the initial weight estimate method is described, including a short overview of the weight estimation tool used and the development of the WERs. In Section III the developed WERs are validated with data of actual aircraft and other advanced concept studies. Further verification include the comparison of sensitivities with the weight estimation tool used to develop the equations. In Section IV a design study is presented using the proposed methodology combined to other classical handbook methods in the assessment of different advanced concepts followed by final comments and conclusion in Section V.

A. Previous Work

Similar previous work in the development of semi-empirical weight methods for advanced configurations is described in this section.

Böhnke[17] developed wing weight equations for conventional aircraft and strut-braced wing aircraft based on the detailed wing weight estimation method from Dorbath[12]. The developed equations are valid for conventional aircraft, forward-swept wing and strut-braced wing. The method from Dorbath considers a detailed sizing of the secondary structure. Although the equations were developed with a design space filling DoE, some limitations apply: 1) the equations are not applicable to high Aspect Ratio (AR) designs (maximum AR is 13 for cantilever aircraft and 17 for SBW); 2) no aeroelastic constraints are applied (e.g. aileron reversal, aeroelastic divergence); and 3) the equations are only applicable to a single material construction.

Bradley[18] developed regression equations based on Finite Element Method (FEM) sizing of Blended Wing Body (BWB) fuselages. Jemitola et al.[19] developed wing WERs for box-wing aircraft based on regression of results from a FEM sizing procedure. Skillen and Crossley[20] present WERs for morphing wing aircraft based on FEM results.

All developments presented have the following points in common: 1) a higher fidelity physics-based method is used as basis in the development of regressions for unconventional concepts, 2) samples covering part of the design space of interest are generated with a suitable DoE approach, and 3) regressions are presented in the form of semi-empirical equations for typical conceptual design applications.

B. Requirements and Objective

The following requirements apply for the initial weight estimate of advanced concepts presented here: 1) simple semi-empirical equations, 2) break the wing weight into main components for better accuracy, 3) consideration of aeroelastic effects, 4) option to consider aluminum and Carbon Reinforced Plastic (CFRP) materials, and 5) equations applicable to a wide range of transport aircraft sizes.

The following aircraft concepts are of interest, including a short description of the potential benefits:

- *Conventional cantilever (Conv.)*: typical cantilever wing construction with unswept or aft swept wings as found in aircraft in service today.
- *Forward-swept wing (FSW)*: forward-swept wings offer the potential of increased laminar flow[21]. Furthermore, the rigid lift distribution is more inboard, requiring less twist in comparison to aft swept wings. The aileron efficiency is expected to increase at high speed, contrary to aft swept wings.

Disadvantages of the concept include: increased static aeroelastic loads and divergence problems, landing gear placement, and reduced trailing edge flaps effectiveness due to higher trailing edge sweep angle.

- *Strut-braced wing (SBW)*: a strut is attached below the wing, additional braces (juries) can be placed as well. Benefits include: wing bending moment relief and potential to reduce the wing weight; possibility to achieve higher aspect ratios at low weight penalties; thinner wings with reduced sweep may enable laminar flow. Disadvantages include: potential increased wing weight due to aeroelastic restrictions, including flutter; additional strut mass and drag; more difficult engine placement.
- *Forward-swept strut-braced wing (FS-SBW)*: associates the benefits of the FSW with the benefits of the SBW, the wing and the strut are swept forward. Since the static aeroelastic loads and divergence are a potential problem for FSW aircraft, the FS-SBW benefits from the bending relief provided by the strut and possibly improved aeroelastic divergence characteristics. The high-wing arrangement required for the strut and its attachment to the fuselage provides a simpler and possibly lighter integration of the main landing gear.

Other concepts such as blended wing-body, box-wing, twin fuselage, C-wing and span-loaders are not considered here. These other configurations are also of interest and could be considered in future activities.

C. Contributions of Current Work

The main contribution of the present paper is a fast weight estimate method for advanced aircraft configurations considering aeroelastic effects, which is sensitive to main design parameters. The method presented forms a simple yet very useful approach for fast assessment and comparison of configurations in early conceptual design. The new wing WERs proposed can also be applied in combination with other design procedures without the need of implementing a complex software or MDO process.

II. Methodology

The weight estimation methodology proposed here is a combination of a modified version of the method from Scott and Nguyen[16] and the wing WERs developed for each concept using a detailed wing weight estimation tool. Note that here focus is placed on improving the wing weight estimation. If other components sensitivities are considered important for a certain study, then more detailed WERs should be developed for these components accordingly.

A. Initial Weight Estimate

The initial weight estimate procedure from Scott and Nguyen[16] assumes that the aircraft Operating Empty Weight (OEW)[a] consists of two groups:

1. *Constant weight*: weight of components that do not scale with the Maximum Take-Off Weight (MTOW). This weight fraction is a function of the design number of passengers.
2. *Variable weight*: weight of components that scale with the MTOW. This group is represented by a fraction of the MTOW.

These group definitions are helpful in conceptual design since they state what the main weight drivers of each component are.

The method from Scott and Nguyen[16] is extended here in two points: 1) the wing weight fraction of MTOW is estimated based on WERs equations developed for each aircraft configuration, and 2) the propulsion weight (engine, installation and nacelle) is estimated based on the engine thrust. This allows the propulsion weight to scale with the aircraft thrust to weight ratio, T/W. The weight group definitions applied here are presented in Table 1.

[a]Note that in this paper the word "weight" is used for the mass in kg, and not for the weight force in N.

Table 1. Weight group definitions.

Group	Variable group	Constant group	Propulsion group	Wing group
Coefficient	Fraction of the MTOW	Weight divided by number of passengers, kg/pax	Weight in newtons divided by engine thrust	Based on WERs
Components	- Tail - Landing gear - Flight controls - Hydraulic & pneumatic - Anti-icing	- Fuselage - APU - Instruments - Electrical - Avionics - Furnishings - Air conditioning - Operator items	- Dry engine - Engine installation - Nacelles - Pylons	- Wing - Strut & juries

The aircraft MTOW is then given by:

$$m_{TO} = \frac{K_c n_{pax,c} + m_{pay}}{1 - K_v - K_w - K_p \cdot (T/W) - K_f} \tag{1}$$

where,

K_c = constant weight group coefficient, kg/pax

$n_{pax,c}$ = number of passengers for constant weight estimation [-]

m_{pay} = design payload weight, kg

K_v = variable weight group coefficient without wing, fraction of MTOW [-]

K_w = wing weight as a fraction of MTOW. Calculated with the WERs from Section II.B [-]

K_p = propulsion weight group coefficient. Total installed propulsion, nacelles and pylons weight divided by the engine thrust (W/T) [-]

K_f = design fuel weight fraction of MTOW [-]

(T/W) = aircraft design thrust to weight ratio at take-off [-]

The definition of the number of passengers for constant weight estimation $n_{pax,c}$ applied here is slightly different than the one given by Scott and Nguyen[16]. Instead of calculating the number of passengers based on different densities for narrow-bodies and wide-bodies as a function of the cabin floor area, here a simple relation is applied:

$$n_{pax,c} = l_f d_f \tag{2}$$

Where, l_f is the total fuselage length (m) and d_f is the maximum fuselage width (m). This definition permits a fast evaluation of the number of passengers and approximates well typical seating capacities.

Data on the constant weight K_c, variable weight K_v, and propulsion weight K_p coefficients are obtained from previous similar designs. The design study presented in Section IV is based on the CeRAS[22] short-range aircraft. The coefficients for this aircraft are calculated and presented in Table 2 for reference. The wing group coefficient is shown for reference only, the actual value is calculated with the WERs developed. Advanced Technology Multipliers (ATM) for EIS in 2045 are also presented according to the method from Scott and Nguyen[16], assuming a composite fuselage. No changes are applied to the propulsion group and variable group coefficient.

Table 2. Group weight coefficients obtained for the CeRAS short-range aircraft[22] including advanced technology multipliers for EIS 2045.

Component	Unit	CeRAS	ATM*
Variable group coefficient, Kv	[-]	0.071	1.00
Constant group coefficient, Kc	[kg/pax]	130	0.85
Propulsion group coefficient, Kp	[-]	0.374	1.00
Wing group coefficient, Kw	[-]	0.105	-

*Advanced technology multiplier for EIS 2045

The wing weight fraction K_w to be applied in Eq. (1) is calculated by:

$$K_w = \frac{m_w}{m_{TO,0}} \tag{3}$$

Where m_w is the wing weight obtained with the WERs form Section II.B and $m_{TO,0}$ is an initial MTOW guess. The initial $m_{TO,0}$ is also applied in the WERs. The $m_{TO,0}$ guess can be based on other aircraft or studies with similar mission requirements and size. The main effect of $m_{TO,0}$ here is to consider for size effects and this can be accomplished with approximate guesses independent of the design parameters. The actual MTOW is obtained with the more accurate Eq. (1).

The design fuel weight fraction K_f is calculated with the method from Ref. 16, which is based on simple application of the Breguet range equation:

$$K_f = \left(1 - K_{ca} e^{-R/B}\right)(1 + K_{rsv}) \tag{4}$$

Where,

R = design range, km

K_{ca} = climb and acceleration aircraft mass fraction (between 0.99 and 0.995)

K_{rsv} = reserve fuel as a fraction of the mission fuel (between 0.25 and 0.10, smaller values for long-range)

B = Breguet factor, $B = \frac{L}{D}\frac{V_{cr}}{c_t}$

L/D = cruise lift-to-drag ratio

V_{cr} = cruise true airspeed, km/h

c_t = engine specific fuel consumption, 1/h

The cruise lift-to-drag ratio is calculated based on the cruise lift coefficient and a parabolic drag polar:

$$\frac{L}{D} = \frac{C_L}{C_{D0} + KC_L^2} \tag{5}$$

The zero-lift drag coefficient is estimated according to the equivalent flat plate equation $C_{D0} = C_f(S_{wet}/S)$. Where C_f is obtained from previous similar designs (about 0.003 for typical transport jets) and the wetted area ratio (S_{wet}/S) is calculated according to Loftin[23]. The induced drag factor is $K = 1/(\pi Ae)$, where the span efficiency factor e is calculated with the Shevell method[24] as presented by Gudmundsson[1].

The engine specific fuel consumption c_t is determined according to similar engines or engine data available.

B. Wing Weight Estimation Relationships

The development of the wing WERs is presented in this section. For each configuration of interest, typical design parameters are selected and a Design of Experiments is performed with a detailed wing weight estimation tool. The wing weight estimated for each sample in the DoE is used in a least squares regression in order to obtain

the WER equations. The WERs are developed for the configurations presented in Section I.B: conventional, FSW, SBW, and FS-SBW. For each configuration, two materials are considered:

- *Aluminum*: Conventional aluminum construction for the wing-box. Upper covers, webs and ribs are made of aluminum 7075. Lower covers are made of aluminum 2024 with an average fatigue allowable.
- *CFRP*: Carbon fiber reinforced plastic (CFRP) for the wing-box. The CFRP wings are built with the T300/5208 graphite epoxy composite[25]. The wing covers are made of 50% fibers in the wing-box center axis direction, 38% fibers in ±45° and 12% fibers perpendicular to the axis. The webs and ribs are made of 12% fibers in the axis direction, 76% fibers in ±45° and 12% fibers perpendicular to the axis. The laminates are always balanced. Therefore, no aeroelastic tailoring effects are considered. A rough estimation of the benefits of aeroelastic tailoring is to reduce the wing weight in about 8% for FSW aircraft.

1. Wing Weight Estimation Tool

The detailed wing weight estimation tool used in the development of the DoE data is described in detail in Ref. 11. Here a short overview of the method is presented.

The wing load carrying structure (covers and spars) is sized according to different load cases and aeroelastic constraints. The load cases include: positive and negative symmetrical maneuvers, quasi-static gusts, 1g fatigue case, roll maneuver, landing and bump on ground. The wing loads are calculated considering static aeroelastic effects with structural flexibility matrices coupled to a simplified Vortex-Lattice Method (VLM). Effects such as the required flight shape and the corresponding jig shape are taken into account. The wing-box is sized at different sections according to strength, buckling and fatigue criteria. Aluminum or composite materials can be considered. Furthermore, static aeroelastic constraints due to aileron efficiency and aeroelastic divergence are considered in the wing-box sizing with a simple optimization method. The weight of non-structural items in the wing-box and the secondary structure are estimated with semi-empirical methods. The aeroelastic method has been validated with MSC Nastran[26]. The complete method is applicable to unconventional aircraft such as SBW and FSW. Comparison of the estimated wing weight for 22 conventional aircraft shows an average absolute error of 10.6%[11].

A typical geometry representation in the wing weight tool is presented in Fig. 1.

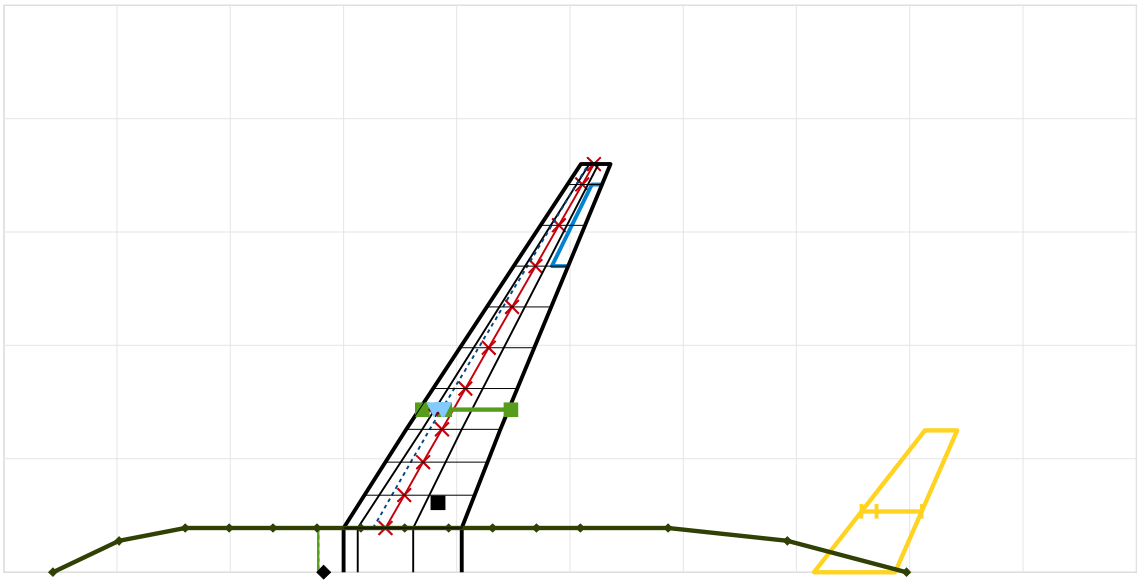

Figure 1. Typical geometry description in the detailed wing weight tool.

2. Equation Form

The first step in the DoE preparation is the definition of the equation form and parameters covering the design space. A compromise between simplicity and inclusion of significant design parameters is desired. Although many other WERs consider the weight of the complete wing structure directly[2,3,8,17], it is decided here to split the wing into main components: covers (skins+stringers), webs plus ribs, secondary structure, and strut plus juries for SBW

aircraft. This breakdown is intended to improve the quality of the WER since each structural component is sized for different conditions and scales differently with the design parameters. The wing WER form is given by:

$$m_w = k_{ail}(m_{covers} + m_{web+ribs}) + m_{sec} + m_{strut} \tag{6}$$

where,

m_{covers} = wing-box covers including skins, stringers and non-optimal weight penalties, kg

$m_{webs+ribs}$ = wing-box spar webs and ribs, including non-optimal weight penalties, kg

m_{sec} = secondary wing structure weight (trailing edge flaps, landing gear attachment, pylon attachments, fixed leading and trailing edges, slats and leading edge devices, spoilers, ailerons, paint, wingtip and miscellaneous), kg

m_{strut} = strut and juries weight. Only applicable to strut-braced wing aircraft, kg

k_{ail} = wing-box weight penalty factor to achieve aileron efficiency constraints. Equal to one for no wing-box weight penalty. See Section II.B.6 for more details.

Note that the wing weight breakdown applied here is the same as in Ref. 11. Regressions are performed separately for m_{covers}, $m_{webs+ribs}$, m_{strut}, and k_{ail}. The secondary wing structure weight is estimated for all concepts with the following equation[11]:

$$m_{sec} = 0.0443 \cdot m_{TO} \tag{7}$$

This is the same equation present in the detailed wing weight method. It presents an average absolute error of 5% and a maximum error of 9% for secondary wing weight data on five aircraft not used in the development of the equation. The factor 0.0443 should be reduced to 0.0338 for small aircraft with simple flap systems. Another advantage of dividing the wing WER into main components equations is that if other secondary wing weight methods are available they can be substituted instead of using the equation above.

The WERs for the covers m_{covers}, webs plus ribs $m_{webs+ribs}$, and strut plus juries m_{strut} have the following form:

$$m_{covers} = k_e \cdot C \cdot m_{TO}^{E_m} (W/S)^{E_{ws}} A^{E_A} (\cos\Lambda)^{E_\Lambda} (t/c)^{E_t} V^{E_V} (1+\lambda)^{E_\lambda} n_z^{E_{nz}} (1-\eta)^{E_\eta} \tag{8}$$

$$m_{webs+ribs} = k_e \cdot C \cdot m_{TO}^{E_m} (W/S)^{E_{ws}} A^{E_A} (\cos\Lambda)^{E_\Lambda} (t/c)^{E_t} V^{E_V} (1+\lambda)^{E_\lambda} n_z^{E_{nz}} (1-\eta)^{E_\eta} \tag{9}$$

$$m_{strut} = k_e \cdot C \cdot m_{TO}^{E_m} (W/S)^{E_{ws}} A^{E_A} (\cos\Lambda)^{E_\Lambda} (t/c)^{E_t} V^{E_V} (1+\lambda)^{E_\lambda} n_z^{E_{nz}} (1-\eta)^{E_\eta} p_{st}^{E_{pst}} \tag{10}$$

Different exponents E and constant C are used for each equation above and for each concept. The parameters are defined as follows,

k_e = engine relief factor [-]. See Table 9

m_{TO} = aircraft maximum take-off weight, kg

W/S = aircraft wing loading at take-off weight. The wing area used for reference is the actual exposed area plus a rectangular area along the fuselage, N/m²

A = wing aspect ratio [-]

Λ = wing sweep angle of the line through the center of the wing-box, deg

t/c = airfoil relative thickness to chord ratio at the wing kink position. The wing kink is at 35% of the span for conventional and FSW aircraft. For SBW and FS-SBW aircraft the kink is defined by η [-]

V = maximum operating speed, equivalent airspeed, m/s

λ = wing taper ratio. Ratio of wingtip chord to wing root chord at fuselage attachment for conventional, FSW and FS-SBW. For aft swept SBW aircraft it is the ratio between the wingtip chord and the chord at the strut attachment along the span. For aft swept SBW the chord between the wing root and the strut attachment position is assumed constant (no taper) [-]

n_z = design positive limit load factor [-]

η = strut position as a fraction of the wing span, only applicable to SBW and FS-SBW [-]

p_{st} = strut parameter, $p_{st} = 1 - \frac{(c_{st}/c)^{0.5}\,\eta^2}{A^{0.5}}$, only applicable to SBW and FS-SBW aircraft [-] c_{st}/c is the ratio of strut chord to wing chord at the wing attachment[11].

The wing-box weight penalty factor to achieve aileron efficiency constraints in Eq. (6) is given by:

$$\begin{aligned} &k_{ail} = \left(\frac{\eta_{ail}}{0.5}\right)^{-1.1} \text{, for conventional and SBW if } \eta_{ail} < 0.5 \\ &k_{ail} = 1 \text{ , for conventional and SBW if } \eta_{ail} \geq 0.5 \\ &k_{ail} = 1 \text{ , for all FSW and FS-SBW} \end{aligned} \tag{11}$$

Where η_{ail} is the aileron efficiency at 67% of the maximum operating airspeed at sea level. The aileron efficiency is defined here as the ratio between the elastic rolling moment coefficient derivative due to aileron deflection and the rigid rolling moment coefficient derivative. The constant -1.1 is obtained empirically as described in Section II.B.6. The aileron efficiency is estimated with a regression similar to the WERs:

$$\eta_{ail} = C \cdot m_{TO}^{E_m} \left(W/S\right)^{E_{ws}} A^{E_A} \left(\cos\Lambda\right)^{E_\Lambda} \left(t/c\right)^{E_t} V^{E_V} \left(1+\lambda\right)^{E_\lambda} n_z^{E_{nz}} (1-\eta)^{E_\eta} p_{st2}^{E_{pst2}} \tag{12}$$

The only differences to Eqs. (8-10) are the absence of an engine relief factor k_e and the usage of a different strut parameter: $p_{st2} = 2 - \eta/\cos^2\Lambda$. Further details about the aileron efficiency and the wing-box weight penalty due to aileron efficiency constraint are given in Section II.B.6.

3. Assumptions in Developing the WERs

The definition of the wing geometry, load conditions and structure layout depends on many more parameters than the ones present in the WERs proposed. Nevertheless, to keep the equations simple and useful for early design, some assumptions must be made. The first assumption is that for typical trades of interest, the parameters present in the WERs are the most relevant for the wing weight. The second is that for other important parameters related to the wing weight, e.g. front and rear spar positions, a set of typical values is assumed.

The assumed airfoil thickness distribution is shown in Fig. 2. The geometry definitions for conventional, FSW and FS-SBW are presented in Fig. 3, the exposed wing is trapezoidal. For aft swept SBWs (Fig. 4) the wing has no taper until the strut attachment position η. The outer wing portion is tapered. The aft swept SBWs constant inboard chord is consistent with the reduced loading due to the strut and can enable reduced manufacturing costs. The same concept is not applied to the forward swept SBW (FS-SBW) in order to keep the leading edge sweep angle low for laminar flow.

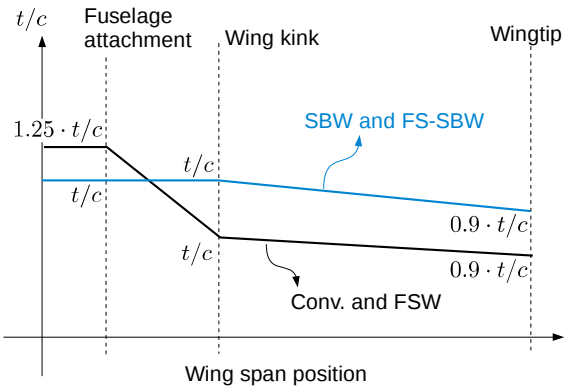

Figure 2. Wing airfoil thickness distribution definition for each concept.

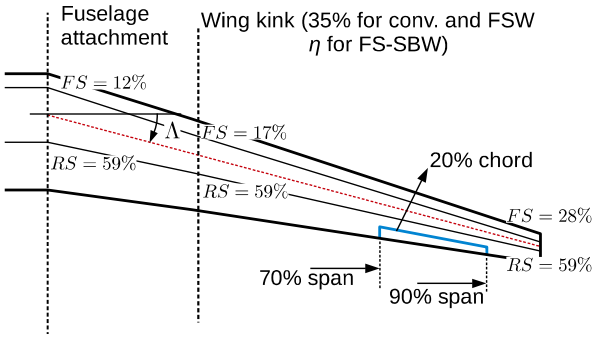

Figure 3. Wing geometry definitions (front and rear spar position, kink, aileron and sweep angle) for conventional, FSW and FS-SBW concepts.

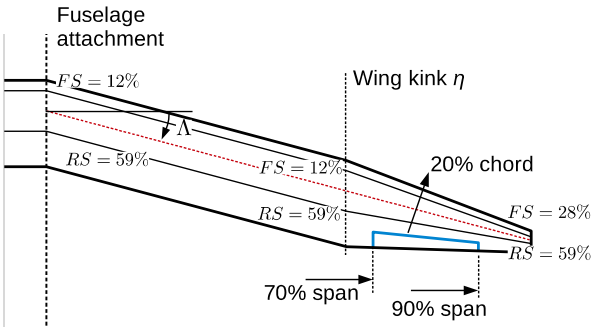

Figure 4. Wing geometry definitions (front and rear spar position, kink, aileron and sweep angle) aft SBW concept.

The following additional assumptions apply:

- The fuselage width (and consequently the wing carry-through box width) is calculated from a fuselage fineness ratio of 9.67. This is an average value for transport aircraft.
- The fuselage length (m) is a function of the MTOW (kg): $l_f = 15.641 \ln(m_{TO}) - 136.41$. Based on data of around 70 transport aircraft. The fuselage length affects the tail position and the aerodynamic center shift due to fuselage aerodynamics. Both effects are important in determining the balancing tail load.
- The aircraft maximum operating Mach number (MMO) is assumed a function of the wing sweep and thickness to chord ratio based on the modified Korn equation[27] for a design lift coefficient of 0.5 and airfoil technology factor of 0.93. $MMO = \frac{0.93}{\cos\Lambda} - \frac{t/c}{\cos^2\Lambda} - \frac{0.5}{10\cos^3\Lambda}$. The maximum value for MMO is 0.92. The MMO is important in the calculation of gust load cases, aerodynamic loading and aeroelastic effects due to its impact on the lift slope coefficient.
- The aircraft maximum zero-fuel weight m_{ZF} is a function of the MTOW (kg): $\frac{m_{ZF}}{m_{TO}} = -0.085 \ln(m_{TO}) + 1.748$, based on data of 70 transport aircraft.
- The aircraft Maximum Landing Weight (MLW) is equal to the MTOW. This is important for the landing cases.
- The design lift distribution at the flight shape is elliptical.
- The minimum material thickness is 1.5 mm for wing-box covers skins, webs and ribs.
- The wing-box covers ratio of skin area to skin plus stringers area is 0.67.

- The ribs spacing (m) is a function of the MTOW (kg). $L_{rib} = 0.089 \ln(m_{TO}) - 0.421$, based on data of a few transport aircraft.
- The aileron is placed from 70% to 90% of the wing span. The aileron chord is 20% of the local chord. This affects the roll maneuver cases and the aileron efficiency requirement.
- A constant airfoil pitching moment coefficient of -0.1 is assumed along the span.
- The wing-box covers stringers pitch (m) is a function of the wing loading (N/m²): $b_{str} = 0.069 \ln(W/S) - 0.478$, this correlation is very approximate and based on data of a few transport aircraft.
- The fatigue allowable (MPa) for aluminum material is a function of the MTOW (kg): $F_{all} = 8.68 \cdot 10^{-5} m_{TO} + 74.7$. The rationale is that for lower MTOW, more life-cycles are required so the allowable is lower. For CFRP wings it is assumed that no fatigue allowable applies.
- The tail area is 25% of the wing area and the tail is placed at 90% of the fuselage length. This is important in determining the balancing tail load and consequently additional lift required on the wing.
- A forward CG position at 15% of the Mean Aerodynamic Chord is used for all load cases.

Assumptions applying only to SBW aircraft:

- The strut is attached to the wing front spar.
- The strut structural box width is 30% of the strut chord.
- The strut airfoil thickness to chord ratio is equal to the wing airfoil t/c plus $0.05/\cos(\Lambda)$, but not greater than 20%. This assumption is justified if the strut is not generating lift in flight (the maximum allowed thickness in transonic conditions for an airfoil is higher if its lift coefficient is zero).
- One additional jury is placed between the strut and the wing.
- The strut sweep angle is equal to the wing sweep angle.
- Independent on the wing material, the strut material is always CFRP with 50% fibers in the strut box axis direction, 38% fibers in ±45° and 12% fibers perpendicular to the axis. The laminate is balanced.

Most of the values and assumptions above are typical for transport aircraft. These assumptions may be considered very crude guesses even for conceptual design purposes. Nevertheless, the intention here is to provide approximate values for a detailed wing weight estimation to be performed. It is further assumed that the sensitivity of the wing weight to many of the assumptions is small. One could include all these parameters as part of the WERs. Nevertheless, this would be not practical for design. All assumptions are listed above for completeness in describing how the WERs are developed. If a very different assumption applies to a certain design study and its effect is expected to be significant, then the equations provided here are likely to produce inaccurate results.

4. Design of Experiments

In order to perform the regressions to define the constant C and the exponents E in the WERs Eqs. (8-10,12), a set of samples is required. A DoE is performed by selecting a design space filling approach. The Latin hypercube [28] is selected for this purpose due to its simplicity and efficiency in covering the design space uniformly. A different set of samples for each concept and material construction is selected, resulting in a total of 8 samples sets (two materials and four concepts). The number of samples applied for each concept and material is: conventional, 50; FSW, 50; SBW, 70; FS-SBW, 70. More samples are applied to the SBW and FS-SBW concepts due to the higher number of parameters. The maximum and minimum values of the WERs parameters is given in Table 3. The samples are generated without any engine attached to the wing. The engine relief factor k_e is added separately as described in Section II.B.7.

Table 3. Wing WERs parameters boundaries.

	m_{TO} [kg]	W/S [N/m²]	A [-]	Λ [deg]	t/c [-]	V [m/s]	λ [-]	nz [-]	η [-]	c_{st}/c [-]
Conventional:										
MIN	20000	3000	8	0	0.08	130	0.10	2.00	-	-
MAX	250000	8000	20	40	0.18	200	0.50	3.00	-	-
Forward swept wing (FSW):										
MIN	20000	3000	8	-25	0.10	130	0.10	2.00	-	-
MAX	250000	8000	16	0	0.18	200	0.50	3.00	-	-
Strut-braced wing (SBW):										
MIN	20000	3000	10	0	0.08	130	0.10	2.00	0.25	0.10
MAX	250000	8000	20	40	0.18	200	0.50	3.00	0.75	0.40
Forward swept strut-braced wing (FS-SBW):										
MIN	20000	3000	10	-25	0.08	130	0.10	2.00	0.25	0.10
MAX	250000	8000	20	0	0.18	200	0.50	3.00	0.75	0.40

5. *Regression Analysis*

All samples are calculated for each configuration and material with the advanced wing weight estimation tool from Ref. 11. For the aft swept concepts (conventional and SBW), the sizing is performed with elastic loads but without the wing-box optimization according to aileron efficiency and divergence constraints. For the forward swept concepts (FSW and FS-SBW) the optimization according to the aeroelastic constraints is active. These different approaches are selected due to the following considerations. For the aft swept concepts, the static aeroelastic loads are usually lower for aircraft with low aileron efficiency (e.g. high aspect ratio and high sweep). This results in different trends for the wing-box weight, making it difficult to capture all effects in a single WER. This is one of the reasons for adding the aileron penalty efficiency factor k_{ail} to the Eqs. (8) and (9). For FSW and FS-SBW the additional weight due to aeroelastic constraints (aeroelastic divergence) occurs with similar trends as for the static aeroelastic loads, which are increased e.g. for more forward swept geometries. Therefore, it is easier to capture the effects in a single WER without the requirement of additional parameters.

The obtained exponents and constants with a least-squares regression for the wing covers, Eq. (8), webs and ribs, Eq. (9), and strut plus juries, Eq. (10), are given in Tables 4, 5 and 6 respectively. The numbers in brackets in the tables are the standard deviation of each exponent and indicate the data scatter for each parameter. A standard deviation that is close to the exponent value or higher indicate parameters with much scatter that are not well represented by the equation. Exponents close to zero indicate possibly unimportant parameters. Here, the presumably "unimportant" parameters are not removed from the equations, so for all concepts the WERs have similar form. Nevertheless, one can quickly identify which parameters are not very important in describing the weight variations. For example, for the covers, m_{TO}, W/S, A, sweep Λ and t/c are important parameters for all configurations (exponents different than zero with very low standard deviation). However, the maximum operating speed V is not very significant for all concepts with exception of the FSW and FS-SBW configurations. This can be identified by the exponents with values close to zero.

Table 4. Wing covers WERs constants and exponents for each concept and material to be applied in Eq. (8). The numbers in brackets correspond to the standard deviation of each exponent.

	C	m_{TO}	W/S	A	Λ	t/c	V	λ	nz	η
Conv Al	1.18E-3	1.305	-0.662	1.464	-1.718	-1.000	0.036	0.367	0.314	-
		(0.005)	(0.011)	(0.012)	(0.042)	(0.014)	(0.025)	(0.035)	(0.027)	-
Conv CFRP	1.17E-4	1.401	-0.638	1.445	-1.245	-1.001	0.065	0.749	0.819	-
		(0.009)	(0.022)	(0.024)	(0.081)	(0.026)	(0.048)	(0.067)	(0.053)	-
FSW Al	2.25E-5	1.367	-1.149	2.158	-5.421	-1.550	0.948	0.738	0.385	-
		(0.026)	(0.070)	(0.091)	(0.604)	(0.117)	(0.138)	(0.189)	(0.143)	-
FSW CFRP	5.14E-5	1.391	-1.067	1.926	-3.731	-1.400	0.694	0.672	0.467	-
		(0.019)	(0.050)	(0.065)	(0.434)	(0.084)	(0.099)	(0.136)	(0.103)	-
SBW Al	1.87E-2	1.231	-0.675	1.190	-1.788	-0.812	-0.020	0.186	0.371	1.484
		(0.012)	(0.027)	(0.038)	(0.098)	(0.032)	(0.060)	(0.086)	(0.066)	(0.025)
SBW CFRP	2.25E-3	1.351	-0.708	1.190	-1.794	-0.724	0.020	0.603	0.886	1.511
		(0.017)	(0.038)	(0.052)	(0.136)	(0.045)	(0.084)	(0.120)	(0.091)	(0.035)
FS-SBW Al	1.12E-3	1.273	-0.871	1.573	-3.743	-1.101	0.478	-0.094	0.497	1.563
		(0.031)	(0.072)	(0.103)	(0.698)	(0.086)	(0.166)	(0.223)	(0.175)	(0.065)
FS-SBW CFRP	5.94E-4	1.309	-0.865	1.556	-3.396	-1.054	0.434	0.218	0.658	1.651
		(0.028)	(0.065)	(0.094)	(0.634)	(0.078)	(0.151)	(0.203)	(0.159)	(0.059)

Table 5. Wing ribs and webs WER constants and exponents for each concept and material to be applied in Eq.(9). The numbers in brackets correspond to the standard deviation of each exponent.

	C	m_{TO}	W/S	A	Λ	t/c	V	λ	nz	η
Conv Al	2.05E-1	1.410	-0.892	0.122	-0.379	0.339	0.080	-0.013	0.392	-
		(0.006)	(0.013)	(0.014)	(0.049)	(0.016)	(0.029)	(0.041)	(0.032)	-
Conv CFRP	1.63E-2	1.447	-0.758	0.265	-0.459	0.167	0.099	0.149	0.523	-
		(0.005)	(0.011)	(0.012)	(0.042)	(0.014)	(0.025)	(0.035)	(0.027)	-
FSW Al	2.34E-1	1.401	-1.112	0.348	-0.643	0.200	0.335	0.135	0.169	-
		(0.011)	(0.030)	(0.039)	(0.258)	(0.050)	(0.059)	(0.081)	(0.061)	-
FSW CFRP	3.25E-2	1.423	-0.991	0.468	-0.734	0.021	0.330	0.195	0.198	-
		(0.010)	(0.028)	(0.036)	(0.240)	(0.047)	(0.055)	(0.075)	(0.057)	-
SBW Al	8.61E+0	1.328	-1.115	0.009	-0.620	0.612	0.052	0.111	0.412	0.442
		(0.014)	(0.033)	(0.046)	(0.119)	(0.039)	(0.074)	(0.105)	(0.080)	(0.030)
SBW CFRP	2.09E-1	1.435	-0.954	0.200	-0.702	0.340	0.016	0.344	0.686	0.726
		(0.008)	(0.018)	(0.025)	(0.064)	(0.021)	(0.040)	(0.057)	(0.043)	(0.016)
FS-SBW Al	4.36E+0	1.308	-1.173	0.185	-1.232	0.435	0.245	-0.081	0.175	0.513
		(0.020)	(0.045)	(0.065)	(0.437)	(0.054)	(0.104)	(0.140)	(0.109)	(0.041)
FS-SBW CFRP	1.31E-1	1.398	-1.039	0.353	-1.005	0.224	0.280	0.328	0.443	0.818
		(0.017)	(0.038)	(0.055)	(0.370)	(0.046)	(0.088)	(0.118)	(0.093)	(0.034)

Table 6. Strut and juries WER constants and exponents for each concept and material to be applied in Eq.(10). The numbers in brackets correspond to the standard deviation of each exponent.

	C	m_{TO}	W/S	A	Λ	t/c	V	λ	nz	η	p_{st}
SBW Al	1.01E-3	1.553	-1.098	0.849	-2.467	0.018	0.098	1.163	1.123	-4.386	46.1
		(0.065)	(0.152)	(0.250)	(0.532)	(0.175)	(0.331)	(0.469)	(0.358)	(0.454)	(6.1)
SBW CFRP	1.01E-3	1.556	-1.107	0.885	-2.516	0.056	0.106	1.307	1.148	-4.295	46.2
		(0.065)	(0.152)	(0.250)	(0.533)	(0.175)	(0.331)	(0.470)	(0.358)	(0.455)	(6.1)
FS-SBW Al	3.59E-6	1.662	-1.370	1.410	-1.605	-0.772	0.944	0.412	0.865	-5.134	54.4
		(0.076)	(0.174)	(0.277)	(1.685)	(0.209)	(0.402)	(0.539)	(0.422)	(0.426)	(5.8)
FS-SBW CFRP	5.03E-6	1.660	-1.319	1.335	-1.196	-0.696	0.854	0.414	0.898	-5.058	53.3
		(0.073)	(0.167)	(0.265)	(1.613)	(0.200)	(0.385)	(0.516)	(0.404)	(0.408)	(5.6)

The constants and exponents for the aileron efficiency (η_{ail}) regression Eq. (12), are presented in Table 7. Further details about the development of this data are presented in Section II.B.6.

Table 7. Aileron efficiency regression constants and exponents for each concept and material to be applied in Eq.(12). The numbers in brackets correspond to the standard deviation of each exponent.

	C	m_{TO}	W/S	A	Λ	t/c	V	λ	nz	η	$p_{st,2}$
Conv Al	3.36E+0	-0.036	0.446	-0.467	1.590	0.375	-0.556	-0.187	0.018	-	-
		(0.019)	(0.044)	(0.048)	(0.165)	(0.054)	(0.098)	(0.069)	(0.108)	-	-
Conv CFRP	1.60E+0	-0.006	0.366	-0.353	1.250	0.305	-0.446	-0.100	0.117	-	-
		(0.016)	(0.038)	(0.041)	(0.140)	(0.046)	(0.083)	(0.059)	(0.091)	-	-
SBW Al	5.70E+2	-0.062	0.456	-0.460	2.115	0.512	-1.270	-0.299	0.296	1.064	-1.973
		(0.022)	(0.050)	(0.069)	(0.508)	(0.059)	(0.120)	(0.160)	(0.120)	(0.227)	(0.445)
SBW CFRP	4.64E+2	-0.011	0.423	-0.342	2.380	0.552	-1.255	-0.075	0.522	1.640	-2.634
		(0.024)	(0.054)	(0.075)	(0.558)	(0.065)	(0.132)	(0.176)	(0.132)	(0.250)	(0.489)

The accuracy of the individual WERs, as well as the complete wing weight estimation with Eq. (6) is presented in Table 8 for all samples used in the development of the equations. The values presented include the average absolute error and the R-squared value. The wing weight estimation accuracy is in the order of 3% for the cantilever concepts (conventional and FSW) and around 7% for the strut-braced wing concepts (SBW and FS-SBW). The lower accuracy obtained with the WERs for the SBW and FS-SBW is due to the complex structural characteristics and the increased number of parameters describing the design space.

Table 8. WERs accuracy for all samples used in the development of each equation.

	Average absolute error					R-squared			
	Covers	Webs+ribs	Strut	Ail. Eff.	Wing total	Covers	Webs+ribs	Strut	Ail. Eff.
Conv Al	1.57%	1.88%	-	5.88%	2.30%	1.000	0.999	-	0.928
Conv CFRP	2.90%	1.57%	-	5.04%	1.91%	0.999	1.000	-	0.915
FSW Al	8.80%	3.50%	-	-	5.41%	0.992	0.998	-	-
FSW CFRP	5.71%	3.30%	-	-	3.48%	0.996	0.998	-	-
SBW Al	4.26%	5.04%	23.87%	7.65%	6.58%	0.997	0.996	0.951	0.866
SBW CFRP	5.77%	2.66%	23.90%	8.54%	6.45%	0.996	0.999	0.951	0.850
FS SBW Al	10.46%	7.17%	25.79%	-	9.41%	0.979	0.989	0.937	-
FS SBW CFRP	9.79%	6.21%	24.91%	-	8.93%	0.984	0.993	0.941	-

6. Aileron Efficiency Factor

Accounting for wing-box weight penalties due to aileron efficiency requirements is difficult since this penalty does not necessary appear to all aircraft. For some aircraft, the wing sized for strength criteria only is already stiff enough to achieve a satisfactory aileron efficiency. To account for this correctly, the method proposed here includes the wing-box weight penalty factor k_{ail} in Eq. (6), which assumes the value of one if enough efficiency is available without additional reinforcements.

As presented in the wing weight tool development[11], the aileron efficiency requirement applied in the wing weight estimation method is to achieve at least 50% of the aileron rigid rolling moment coefficient at 67% of the maximum operating speed at sea level, V. The wing-box weight penalty factor k_{ail} is then assumed here to be a function of the ratio between the actual aileron efficiency at 67% V and 50% efficiency, Eq. (11), repeated here for convenience:

$$\begin{aligned} k_{ail} &= \left(\frac{\eta_{ail}}{0.5}\right)^{-1.1} \text{, for conventional and SBW if } \eta_{ail} < 0.5 \\ k_{ail} &= 1 \text{ , for conventional and SBW if } \eta_{ail} \geq 0.5 \\ k_{ail} &= 1 \text{ , for all FSW and FS-SBW} \end{aligned} \tag{11}$$

Where η_{ail} is the aileron efficiency at 67% V. The aileron efficiency is estimated with Eq. (12) in a regression similar to the covers and webs WERs. The exponents and constants in Table 7 are obtained as follows: the exponents for covers, webs and ribs, and strut plus juries presented in Table 4 to Table 6 are calculated with the wing weight tool with the aileron efficiency constraint turned off. Therefore, the aileron efficiency at 67% V is allowed to be below 50%. The obtained aileron efficiency for each sample is used in a regression analysis similar to the other wing weight components, giving the constants and exponents from Table 7. Note that only configurations with unswept or aft swept wings are considered, as it is assumed that no aileron efficiency problems occur for forward-swept wing aircraft.

To determine the constant -1.1 in Eq. (11), the same samples used in the DoE are analyzed with the wing weight tool in the "optimization" mode. The optimization mode increases the wing-box stiffness (and consequently the weight) at different stations along the span to satisfy the aileron efficiency constraint. The aileron penalty factor k_{ail} is then calculated for each sample from the ratio between the wing-box weight with aileron efficiency constraint and without. The penalty factor k_{ail} is plotted as a function of the aileron efficiency (without optimization) ratio to 0.5, $(\eta_{ail}/0.5)$. The result is shown in Figure 5 for each configuration and material. A similar trend is observed for conventional and SBW configurations with different material constructions. The coefficient -1.1 in Eq. (11) is obtained from regression analysis of all points in Figure 5. Note that the scatter in the data increases for very low aileron efficiencies.

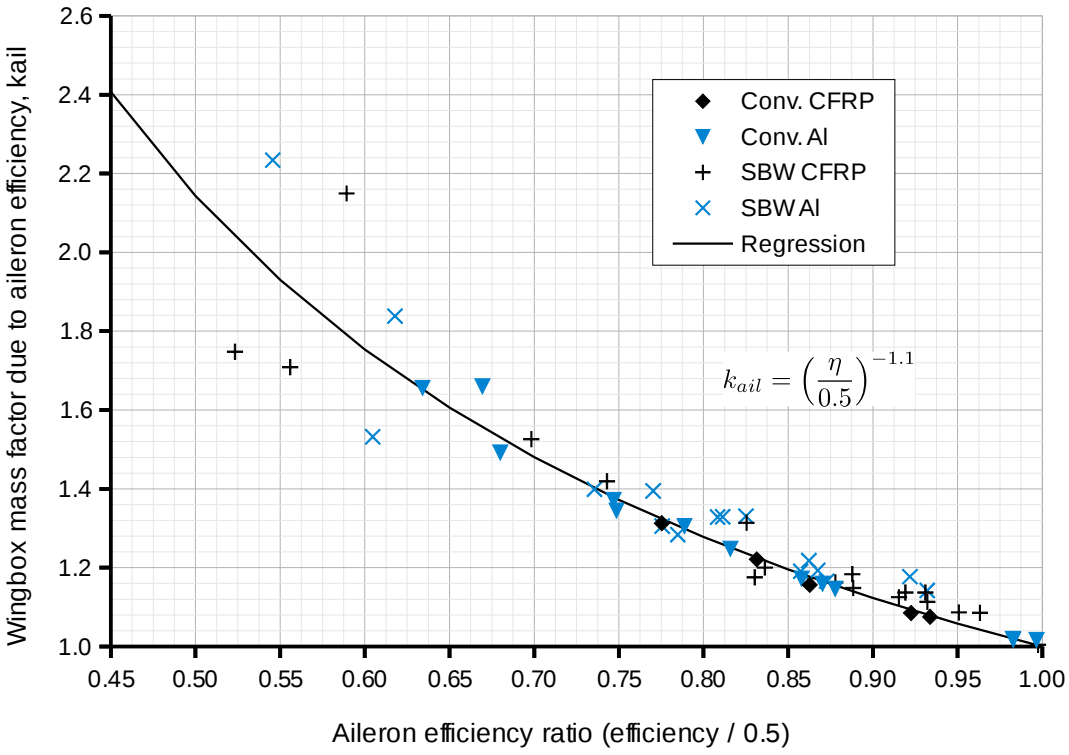

Figure 5. Wing-box weight factor due to aileron efficiency requirement.

7. Engine Relief Factor

The engine relief factor in Eqs. (8-10) is determined as follows. A total of 20 samples covering the same design space defined in Table 3 are generated and analyzed three times: 1) without engine, 2) with two engines, and 3) with four engines. The weight ratio between the results with engine relief and without for each sample is calculated separately for the covers, webs plus ribs, and strut. The average values for all 20 samples are selected and applied as the parameter k_e in the WERs. The results are presented in Table 9 for each concept and material.

The engine y-position along the span is 1.38 times the fuselage diameter for two engines. For four engines, the inner engine y-position is 1.76 times the fuselage diameter and the outer engine is 3.38 times the fuselage diameter. These values are based on statistical data of transport aircraft. The installed engine weight plus pylon and nacelle is based on a very approximate statistical function of the MTOW ($m = 0.123 m_{TO}^{-0.079}$ for two engines, $0.095 m_{TO}^{-0.135}$ for four engines). It is observed that the reduction in wing weight due to engine relief is more effective for FSW aircraft. SBW and FS-SBW wings benefit less from the relief due to the low internal loads obtained with the strut relief.

Table 9. Engine relief factor for each concept and material.

	Covers		Webs+Ribs		Strut+Juries	
Configuration	2 eng.	4 eng.	2 eng.	4 eng.	2 eng.	4 eng.
Conv CFRP	0.985	0.914	0.969	0.909	-	-
Conv Aluminum	0.988	0.929	0.975	0.930	-	-
FSW CFRP	0.963	0.878	0.953	0.887	-	-
FSW Aluminum	0.962	0.885	0.956	0.907	-	-
SBW CFRP	0.990	0.953	0.984	0.912	0.945	0.864
SBW Aluminum	0.996	0.969	0.990	0.944	0.947	0.866
FS-SBW CFRP	0.988	0.939	0.991	0.915	0.938	0.858
FS-SBW Aluminum	0.989	0.957	0.991	0.937	0.938	0.865

III. Validation

A. Conventional Aircraft

The WERs presented here are intended for advanced concepts. No data is available on "real" wing weights for FSW, SBW, or FS-SBW aircraft. Nevertheless, for conventional aircraft it is possible to validate the proposed WER. A consistent reference for this purpose is the report by Beltramo et al.[8], which presents wing weight data on many conventional aircraft and includes the development of a typical wing WER. The validation data consists of 15 transport aircraft and 6 military transports, all with aluminum construction.

The results are presented in Fig. 6 including results obtained with the detailed wing weight tool used in the development of the WERs. The wing weight tool results are presented to verify the regression accuracy. As an example of the accuracy obtained with other typical WERs, the results obtained with the wing WER proposed by Beltramo et al.[8] are also presented. For most aircraft, the absolute errors are below 20% and the WER presented here has a comparable accuracy to the WER from Ref. 8. The exceptions are the military transporters C-130A and C-130E, which have also been identified in Ref. 8 as outliers.

Three points are important to notice. First, the wing weight tool[11] was not calibrated with the data from Ref. 8 but with only few aircraft from York and Labell[15] (B737-200, B727-100, B747, G-159 and G-1159). Therefore, the accuracy achieved with the other 21 aircraft here reassures the robustness of the method and the consequent WERs developed. Second, the differences between the WER from this paper and the wing weight tool used to generate them are small for most aircraft. The only exception is the Citation 500. The WER predicts a weight 20% lower than the weights tool. This aircraft is nevertheless well outside the boundaries of the DoE performed due to its smaller size. Third, many aircraft presented in Fig. 6 have some parameters outside the boundaries defined in the Design of Experiments of the WERs (see Table 3). These parameters are typically aspect ratios lower than 8 and/or take-off weight below or above the limits. Therefore, small extrapolations on the parameters seem to still produce acceptable results.

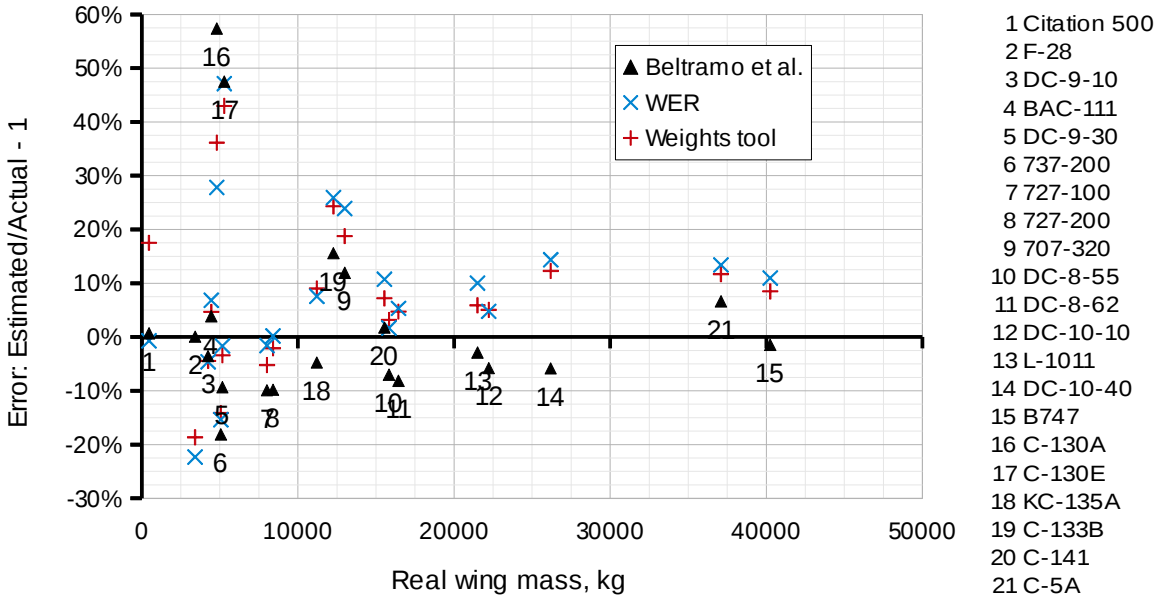

Figure 6. Conventional aluminum WER validation with conventional aircraft data. Average absolute error: Beltramo et al. 11%, WER 12.2%, Wing weight tool 12.4%.

B. Unconventional Aircraft

The validation of the equations for unconventional aircraft is difficult since no jet transport aircraft representative of the configurations presented here (FSW, SBW or FS-SBW) has been built. One option is to compare the results with data on detailed studies of these concepts. This approach enables only approximately the evaluation of the WERs correctness due to the high uncertainty on the detailed studies as well.

This section presents the verification of the WERs for unconventional concepts in comparison to other detailed studies from the literature. For all concepts, the results obtained with the wing weight estimation tool used to develop the WERs are also presented for the parameterization and assumptions applied here in order to verify the regressions accuracy.

The input data for the WERs on the unconventional configurations used in this section is presented in Table 10. The results are presented in Table 11. Discussion of each configuration is presented in the sections below.

Table 10. Input parameters used in the WER verification with unconventional concepts. FSW data from Ref. 29 and SBW from Ref. 30.

	m_{TO} [kg]	W/S [N/m²]	A [-]	Λ [deg]	t/c [-]	V [m/s]	λ [-]	nz [-]	η [-]	c_{st}/c [-]
FSW	73365	5452	9.71	-20.0	0.130	180	0.30	2.5	-	-
SBW	68040	4866	19.56	12.5	0.125	165	0.35	2.5	0.58	0.41

Table 11. WER verification with unconventional concepts results. Reference FSW data from Ref. 29 and SBW from Ref. 30.

	Ref.	WER		Wing weight tool	
Forward swept wing (FSW) – aluminum:					
Wingbox	5895	6598	(+11.9%)	6096	(+3.4%)
Strut-braced wing (SBW) – CFRP :					
Wingbox	3615	3623	(+0.2%)	3500	(-3.2%)
Skins+stringer	2840	2911	(+2.5%)	2852	(+0.4%)
Spars+ribs	775	712	(-8.1%)	648	(-16.4%)
Strut+Juries	484	1017	(+110.2%)	966	(+99.5%)

1. Forward Swept Wing

The FSW concept has been studied at the DLR in the last years. Klimmek[29] presents a detailed sizing procedure for a FSW aircraft in Nastran. The wing-box is modeled with a detailed box model and several sizing constraints and load cases. An optimization process in MSC Nastran is considered for sizing and wing weight estimation. The wing is sized according to strength, fatigue, buckling, and aeroelastic divergence constraints. The wing is made of aluminum material. Further information on the aircraft is presented in Table 10.

The results are shown in Table 11 and compare favorably. The wing-box mass as predicted by the WER is close to the wing weight tool, confirming the regression accuracy. Although the difference in the estimated wing weight relative to Ref. 29 is small, it is important to keep in mind the uncertainty present in the weight estimation of the unconventional concept considered.

2. Strut-Braced Wing

The SBW study by Boeing in the SUGAR project[30] includes a detailed wing weight estimation for a SBW transport aircraft. The weight estimation is based on a detailed Nastran optimization with several load cases and sizing constraints, being a good test for comparison of the WERs proposed here. The wing-box covers (skin+stringers), webs and ribs, and strut and juries from Ref. 30 with consideration of flutter constraint are used for this purpose (Table 2.26 from Ref. 30, column F). The input data used in the WER is presented in Table 10. The results are presented in Table 11, including results obtained with the wing weight tool[11] with the same parameterization applied in the WERs development[*]. The WER used is for CFRP material.

The following conclusions apply to the results: 1) the wing-box weight estimated with the WER and with the wing weight tool is close to the results from Ref. 30, 2) the differences between the WERs and the wing weight tool are below 10% for all components, confirming the regression's accuracy, and 3) higher differences to the SUGAR results occur for the strut and juries due to the different material (the strut weight is very sensitive to the elastic modulus) and assumptions applied (e.g. the strut in the SUGAR design is not of constant chord, here a constant chord is assumed).

The interpretation of the results is nevertheless approximate due to the uncertainties in the results presented here and in Ref. 30 since no real aircraft is available for comparison. Furthermore, the WERs developed here are based on different materials, sizing assumptions and slightly different geometry parameterization than Ref. 30. Nevertheless, in early conceptual design not much detailed data is available and the similar results here give more confidence in the WERs proposed.

C. Sensitivity Verification

In the design study presented in Section IV, 16 different concepts are designed for a short-range mission. As part of the verification of the WERs developed, the wing weight sensitivities obtained for each concept are analyzed. All WERs equation parameters are varied ±10% and ±20% around each point design. The % changes in the wing weight

[*]Note that the results obtained with the wing weight tool are slightly different than the ones in Ref. 11 due to the parameterization applied here, different material properties and updated non-optimal wing weight correction factors.

(including strut) are calculated once with the WERs presented here and once with the weight tool used to develop them. The results are presented in Fig. 7. Note that here only the results for CFRP construction and unconstrained span designs are presented. The results for the other concepts are similar or with better agreement.

In general, similar trends are observed with the WERs and the detailed wing weight tool. Strong non-linear trends such as due to the maximum operating speed (VMO) and strut span position η (both SBW and FS-SBW) are captured but with lower accuracy than other parameters, e.g. aspect ratio or MTOW.

Since the point designs presented here consist of the unconstrained span cases, they represent very extreme design conditions. The results are close to or above the maximum aspect ratio and other parameters possible for the method, including aileron sensitivity and wing divergence constraints. This is a worst case scenario validation of the sensitivities. The sensitivities for constrained span designs are more accurate for many parameters. Nevertheless, it is important to keep in mind the limitations of the regressions in capturing strong non-linear effects in the extremes of the design space.

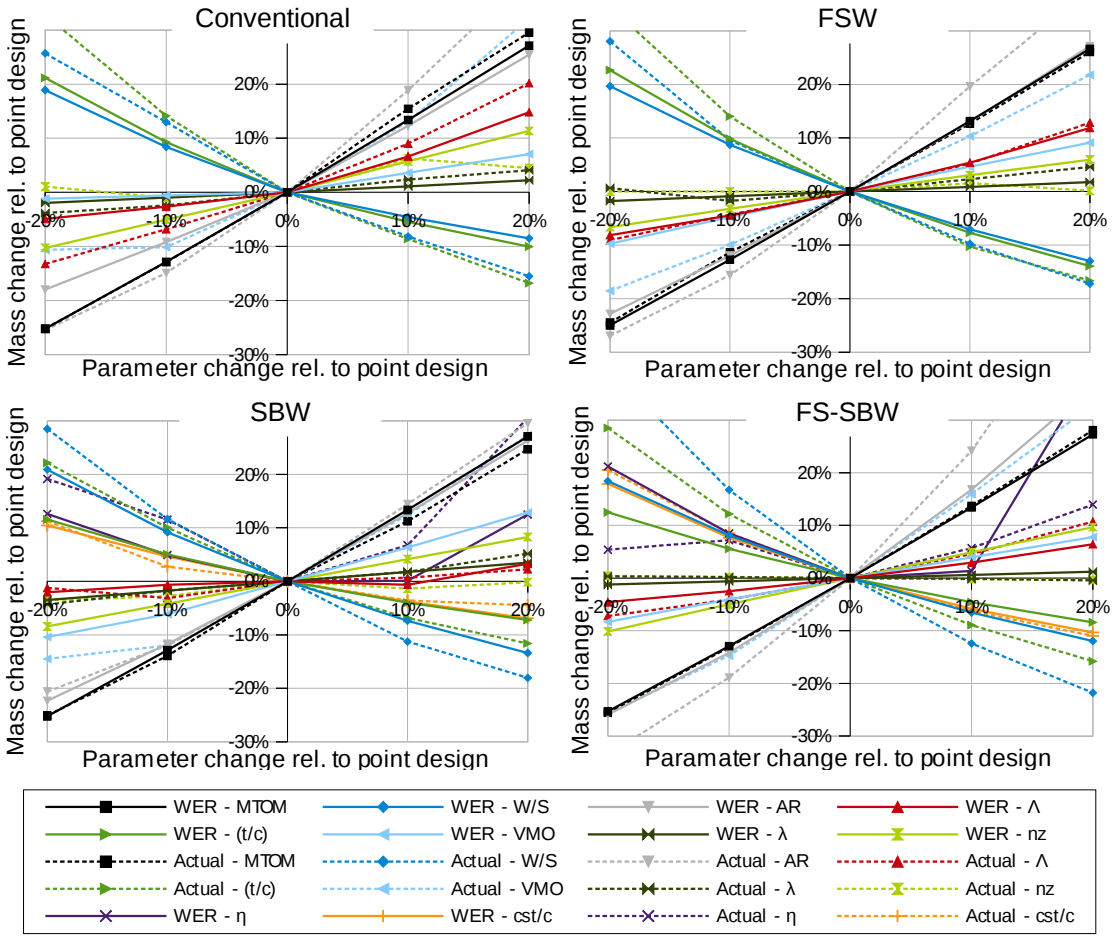

Figure 7. Wing weight sensitivity verification for the point designs from Section IV. Only the point designs with CFRP construction and unconstrained span are presented. Dashed lines results are obtained with the wing weight tool used in the development of the WERs.

IV. Design Study

A conceptual aircraft design study is performed to illustrate the application and benefits of the method. The study consists of a typical activity in conceptual design where different concepts are being considered for a design mission. Usually, when many concepts are being compared, there is no time or resources to analyze each concept in detail. Therefore, designers rely mostly on approximate estimates or expert judgment. With the availability of the

initial weight estimate method proposed here, very fast estimates are possible within the typical time and resource constraints.

A. Design Study Requirements

The design study consists of the comparison of different concepts for the mission requirements of the CeRAS short-range configuration[22]. The top level aircraft requirements are shown in Table 12.

Table 12. Design study top level aircraft requirements.

Requirement	Value
Design cruise speed	Ma = 0.78
Design number of passengers	150
Passenger+luggage mass	90.7 kg
Design range	≥ 2750 nm
Approach speed, MLM, ISA 0m +15°C	≤ 71 m/s
Maximum span for airport compatibility	≤ 36 m
Take-off field length, MTOM, ISA 0m +15°C	≤ 2200 m
Second segment climb gradient, OEI	≥ 2.4%
Climb rate @ top of climb	≥ 300 ft/min
Maximum operating speed	180 m/s EAS
Design limit load factor	2.5

This is a typical short-range aircraft design mission (similar to aircraft such as the A320 and B737). The objective of the study is to compare the potential of each concept (conventional, FSW, SBW and FS-SBW) in reducing fuel burn. The EIS is 2045 and the design objective is to minimize the fuel consumption for the given mission. Two sets of configurations will be considered: 1) respecting the span gate restriction of 36 m, and 2) without span restriction. Furthermore, it is of interest to compare different materials for the wing structure: aluminum or CFRP. All aircraft have aft mounted engines to facilitate the integration of high bypass engines and to enable future improved versions with newer engines. The baseline configuration representing conservative technology development until 2045 is a conventional aircraft with aluminum wings and respecting the span constraint. All results are presented relative to this baseline.

B. Design Methodology

The weights of all concepts are estimated with the initial weight estimate presented here. The weight coefficients and ATMs from Table 2 are applied. A constraint analysis similar to the one proposed by Loftin[23] is used for performance design. The constraint analysis is extended to include the following requirements: 1) Top-of-Climb (TOC) minimum climb rate of 300 ft/min, 2) cruise transonic drag below 10 drag counts, and 3) no buffet at cruise altitude and 1.3g flight. The transonic drag is estimated with the modified Korn equation presented by Mason[27].

All these methods consist of a few analytical equations that can readily be implemented in spreadsheet software according to the design study requirements. An optimization algorithm is used to find minimum fuel consumption solutions respecting the design restrictions. This combination of semi-analytical methods, although very simple, forms a very useful tool for fast assessment of concepts and design requirements.

Assumptions specific to each concept are:

- *Conventional*: no laminar flow, typical high-lift devices.
- *FSW*: laminar flow on 50% of the wing surface, no leading edge devices.
- *SBW*: laminar flow on 30% of the wing surface, no leading edge devices. Fuselage weight increased by 7% due to high-wing configuration.
- *FS-SBW*: laminar flow on 50% of wing surface, no leading edge devices. Fuselage weight increased by 7% due to high-wing configuration.

For all aircraft, an advanced high bypass ratio turbofan engine for EIS 2045 is considered (TSFC = 0.53 1/h). The engine is scaled to the design thrust but the TSFC is held constant.

The design procedure consists in optimizing for minimum fuel burn according to the top level aircraft requirements and constraint analysis restrictions. The following design variables are used in the optimization: 1) wing loading, W/S; 2) thrust to weight ratio, T/W; 3) wing aspect ratio, A; 4) airfoil thickness to chord ratio at kink section, t/c; 5) sweep angle at 50% chordline; and 6) initial cruise altitude, ICA. Furthermore, for the SBW concepts the following variables are also considered: 7) strut position along the span, η; 8) strut chord ratio to wing chord at attachment position, c_{st}/c.

The taper ratio is fixed as $\lambda = 0.25$ for the conventional and FSW configurations, and $\lambda = 0.4$ for the SBW and FS-SBW designs.

C. Results and Discussion

The minimum fuel consumption designs for each configuration are shown in Table 13 (span constrained designs) and Table 14 (no span constraint). The baseline aircraft (conventional, aluminum, 36 m span constraint) is presented in the first column of Table 13. The design is very similar to the CeRAS aircraft[22], but with a slightly higher sweep angle and increased airfoil thickness. This baseline achieves a 24% reduction in fuel consumption in comparison to the EIS 2000 CeRAS short-range aircraft. This is mostly due to the improved engine performance and weight technology factors. An overview of the geometry of each sized aircraft (only CFRP designs) is shown in Fig. 8.

Several points of interest can be identified in the results. The minimum fuel consumption with constrained span is obtained with a FS-SBW design. The difference between aluminum or CFRP material is very small for this configuration (2% fuel weight). The FSW with CFRP wing is the next concept with lowest fuel burn, followed by the SBW, both with constrained span. The MTOW and OEW are nevertheless lower for the SBW concept, also associated with lower weight growth factors. The benefit in using CFRP is small for the SBW concepts with constrained span (2% change in fuel weight), but it is significant for the FSW concept (9% lower fuel weight than the equivalent aluminum concept). With constrained span, FSW, SBW and FS-SBW concepts tend to lower wing loadings in comparison to conventional concepts due to the absence of leading edge devices in order to achieve laminar flow. This is also associated with lower aspect ratios due to the constrained span effect.

With constrained span, all reductions in MTOW are directly associated to a higher aspect ratio at constant wing loading. This can be seen by comparing the conventional CFRP and aluminum concepts. Both have very similar design parameters, except for the aspect ratio, which is higher for the CFRP design. Since the aircraft is lighter, the wing area is smaller for a constant W/S and a higher aspect ratio is achievable with constrained span.

The FS-SBW achieves, for constrained span, the lowest fuel consumption due to the synergy of the following effects: the fuel consumption is lower due to the laminar flow on the wing, the wing weight is reduced due the strut bending relief and the lower overall MTOW, the lower MTOW enables a higher aspect ratio at constant wing loading.

For aircraft with unconstrained span, the minimum fuel consumption is also achieved with the FS-SBW concept. The next lowest fuel burn concepts are then the SBW and the conventional aircraft, both with CFRP wings. Interestingly, the fuel consumption benefit is similar between the SBW and the conventional concept for unconstrained span. The SBW advantage appears in the lower OEW and weight growth factor.

The FSW aircraft with unconstrained span does not achieve similar reductions in fuel burn as for the constrained span case. This is due to the difficulty in increasing the wing span without adding high weight penalties due to aeroelastic effects.

The highest improvement between unconstrained and constrained span similar concepts is achieved by the conventional CFRP design; the fuel burn is 14% lower for unconstrained span. This is due to the increased benefit of applying CFRP to cantilever wings of long span. Similar improvement is also seen for the SBW concepts.

Concerning the active constraints, the wing loading is sized by the approach speed requirement and the thrust to weight ratio at the second segment climb for the constrained span designs. The unconstrained span designs tend to have lower wing loadings and lower thrust to weight ratios. The active constraint is the climb rate at TOC for most unconstrained span designs, this is due to the high optimal initial cruise altitude (ICA).

The tables also show the wing weights estimated with the WERs from this paper and the weight estimated with the detailed wing weight tool from Ref. 11. The results are very similar among the two methods for all concepts. The highest error occurs for the FS-SBW CFRP concept with unconstrained span, -14%. Similar accuracy is verified for the aileron efficiency estimate with Eq. (12).

A remark on the consistency of the results for the SBW concept is necessary. The SBW concepts optimized here have high aft sweep angles, comparable to the conventional cantilever configurations. It is therefore important to verify the sensitivities associated with the sweep angle, otherwise the assumption of laminarity is not justified for the SBW in comparison to the conventional configurations. This verification is nevertheless outside the scope of this work.

Table 13. Design study summary, configurations with span restriction of 36 m.

Configuration	Conv.	Conv.	FSW	FSW	SBW	SBW	FS-SBW	FS-SBW
Span restriction	Yes	Yes	Yes	Yes	Yes	Yes	Yes	Yes
Wing material	Aluminum	CFRP	Aluminum	CFRP	Aluminum	CFRP	Aluminum	CFRP
Aspect ratio	10.90	11.38	8.70	9.26	9.62	9.62	9.85	10.05
T/W	0.311	0.302	0.317	0.304	0.312	0.303	0.296	0.292
W/S [N/m²]	5327	5264	4400	4356	4409	4392	4341	4327
t/c	0.126	0.128	0.117	0.121	0.126	0.116	0.096	0.096
Sweep angle 50% [°]	29.9	30.2	-22.7	-25.0	27.2	23.9	-18.4	-18.1
Initial Climb Altitude [ft]	39754	39882	39093	40483	41119	40758	41868	41667
Strut span position	-	-	-	-	0.70	0.51	0.70	0.70
Strut chord ratio, cst/c	-	-	-	-	0.26	0.16	0.34	0.33
MTOM [kg]	64580	60907	66585	61984	60534	60298	58233	56853
Δ MTOM to baseline	(+0.0%)	(-5.7%)	(+3.1%)	(-4.0%)	(-6.3%)	(-6.6%)	(-9.8%)	(-12.0%)
OEM [kg]	36870	34202	39384	36059	33832	33887	32914	31890
Δ OEM to baseline	(+0.0%)	(-7.2%)	(+6.8%)	(-2.2%)	(-8.2%)	(-8.1%)	(-10.7%)	(-13.5%)
Design fuel mass [kg]	**14102**	**13097**	**13593**	**12317**	**13093**	**12802**	**11711**	**11355**
Δ Fuel to baseline	**(+0.0%)**	**(-7.1%)**	**(-3.6%)**	**(-12.7%)**	**(-7.2%)**	**(-9.2%)**	**(-17.0%)**	**(-19.5%)**
Growth factor	1.626	1.534	1.677	1.561	1.493	1.487	1.436	1.402
Wing span [m]	36.0	35.9	35.9	35.9	36.0	36.0	36.0	36.0
Wing area [m²]	118.9	113.5	148.4	139.6	134.7	134.7	131.6	128.9
Wing mass, WER [kg]	8206	6424	10201	8036	5264	5567	5134	4439
Wing mass, detailed [kg]	8098	6253	9909	7851	5396	5077	5300	4664
Difference wing weight	(+1.3%)	(+2.7%)	(+2.9%)	(+2.4%)	(-2.5%)	(+9.7%)	(-3.1%)	(-4.8%)
Ail. Eff., WER	0.674	0.695	-	-	0.457	0.486	-	-
Ail. Eff., detailed	0.661	0.695	-	-	0.510	0.496	-	-
Difference Ail. Eff.	(+2.0%)	(-0.0%)	-	-	(-10.3%)	(-1.9%)	-	-
L/D @ cruise	17.3	17.6	18.7	19.3	17.5	17.9	19.0	19.2
CL @ cruise	0.659	0.655	0.527	0.558	0.582	0.570	0.594	0.587
Take-off lift coefficient	2.20	2.20	1.83	1.83	1.83	1.83	1.83	1.83
Landing lift coefficient	2.80	2.80	2.33	2.33	2.33	2.33	2.33	2.33
TOFL [m]	2057	2091	2001	2062	2035	2088	2114	2135
Approach speed [m/s]	71.0	70.8	71.0	71.0	71.0	71.0	71.0	71.0
Sec. segment climb rate	2.40%	2.40%	2.40%	2.40%	2.65%	2.40%	2.40%	2.40%
Climb rate TOC [ft/min]	376	328	688	523	300	301	300	300

Table 14. Design study summary, configurations without span restriction.

Configuration	Conv.	Conv.	FSW	FSW	SBW	SBW	FS-SBW	FS-SBW
Span restriction	No	No	No	No	No	No	No	No
Wing material	Aluminum	CFRP	Aluminum	CFRP	Aluminum	CFRP	Aluminum	CFRP
Aspect ratio	14.03	17.08	9.31	11.39	16.82	18.37	14.56	15.54
T/W	0.312	0.312	0.299	0.266	0.302	0.301	0.289	0.295
W/S [N/m²]	3440	3211	3897	4049	3896	3683	3682	3448
t/c	0.135	0.135	0.118	0.123	0.142	0.143	0.105	0.109
Sweep angle 50% [°]	30.5	31.9	-22.8	-25.0	35.0	35.3	-22.4	-24.0
Initial Climb Altitude [ft]	47003	49633	41205	41410	46272	47444	46399	48226
Strut span position	-	-	-	-	0.70	0.66	0.70	0.70
Strut chord ratio, cst/c	-	-	-	-	0.40	0.40	0.40	0.40
MTOM [kg]	69168	65290	68898	63754	63078	62167	61327	59972
Δ MTOM to baseline	(+7.1%)	(+1.1%)	(+6.7%)	(-1.3%)	(-2.3%)	(-3.7%)	(-5.0%)	(-7.1%)
OEM [kg]	42855	40562	41881	38418	38024	37692	37099	36326
Δ OEM to baseline	(+16.2%)	(+10.0%)	(+13.6%)	(+4.2%)	(+3.1%)	(+2.2%)	(+0.6%)	(-1.5%)
Design fuel mass [kg]	**12705**	**11120**	**13409**	**11727**	**11446**	**10868**	**10620**	**10038**
Δ Fuel to baseline	**(-9.9%)**	**(-21.1%)**	**(-4.9%)**	**(-16.8%)**	**(-18.8%)**	**(-22.9%)**	**(-24.7%)**	**(-28.8%)**
Growth factor	1.742	1.644	1.735	1.606	1.556	1.533	1.512	1.479
Wing span [m]	52.6	58.4	40.2	41.9	51.7	55.2	48.8	51.5
Wing area [m²]	197.2	199.5	173.4	154.5	158.8	165.6	163.4	170.6
Wing mass, WER [kg]	13292	11730	12714	10972	9209	9072	8901	8250
Wing mass, detailed [kg]	14264	12941	12996	11482	9099	8567	9637	9616
Difference wing weight	(-6.8%)	(-9.4%)	(-2.2%)	(-4.4%)	(+1.2%)	(+5.9%)	(-7.6%)	(-14.2%)
Ail. Eff., WER	0.500	0.500	-	-	0.405	0.395	-	-
Ail. Eff., detailed	0.467	0.433	-	-	0.404	0.423	-	-
Difference Ail. Eff.	(+7.1%)	(+15.6%)	-	-	(+0.2%)	(-6.5%)	-	-
L/D @ cruise	21.1	23.1	19.8	21.1	21.4	22.4	22.6	23.5
CL @ cruise	0.603	0.639	0.517	0.542	0.659	0.659	0.627	0.641
Take-off lift coefficient	2.20	2.20	1.83	1.83	1.83	1.83	1.83	1.83
Landing lift coefficient	2.80	2.80	2.33	2.33	2.33	2.33	2.33	2.33
TOFL [m]	1321	1234	1877	2189	1856	1762	1833	1685
Approach speed [m/s]	57.7	56.2	67.0	68.8	67.6	65.9	66.0	64.0
Sec. segment climb rate	4.44%	5.41%	2.40%	2.40%	5.10%	5.43%	4.31%	4.82%
Climb rate TOC [ft/min]	300	300	472	300	300	300	300	300

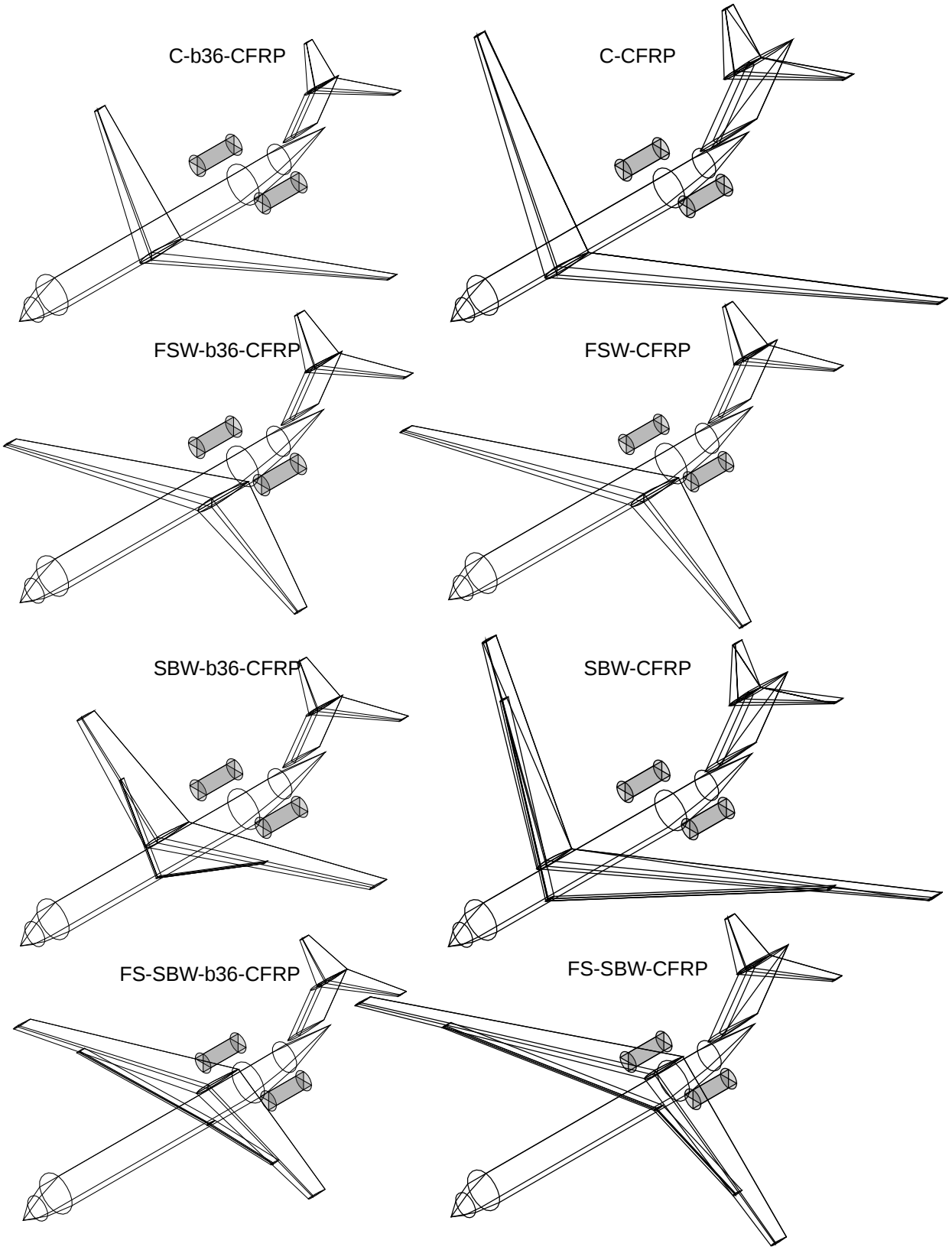

Figure 8. Overview of sized concepts.

V. Conclusion

The method and WERs presented in this paper allow fast assessment of concepts, technologies, requirements and initial aircraft sizing. The complexity is kept to the level of handbook methods while allowing advanced concepts and static aeroelastic effects to be accounted early in the design. The validation of the WERs proposed shows good accuracy for conventional aircraft. Validation for unconventional concepts is difficult due to the uncertainties involved. Nevertheless, the comparison to other detailed studies presented gives increased confidence in the usefulness of the WERs. The design study presented illustrates how important knowledge can be obtained with simple handbook methods for advanced concepts. A promising concept (forward-swept strut-braced wing) is identified. Further detailed studies should be performed in order to investigate its potential, including a detailed evaluation of its aeroelastic characteristics.

Although the results presented are promising, it is important to consider that the method presented here is not intended for detailed studies. It is nevertheless expected that main trades are captured within the accuracy expected for conceptual design.

Future potential developments include the extension to other aircraft configurations and inclusion of flutter requirements in the wing weight estimation.

References

[1]Gudmundsson, S., *General Aviation Aircraft Design: Applied Methods and Procedures*, Elsevier, Oxford, 2014.

[2]Nicolai, L. M., and Carichner, G. E.., *Fundamentals of Aircraft and Airship Design: Volume 1 - Aircraft Design*, AIAA Education Series, AIAA, Reston, 2010.

[3]Raymer, D. P., *Aircraft Design: A Conceptual Approach*, 4th ed., AIAA Education Series, AIAA, Reston, 2006.

[4]Torenbeek, E., *Synthesis of Subsonic Airplane Design*, Delft University Press, Delft, 1982.

[5]Bradley, M. K., and Droney C. K., "Subsonic Ultra Green Aircraft Research: Phase I Final Report," NASA/CR-2011-216847, 2011.

[6]Piperni, P., DeBlois, A., and Henderson, R., "Development of a Multilevel Multidisciplinary-Optimization Capability for an Industrial Environment," *AIAA Journal*, Vol. 51, No. 10, 2013, pp. 2335-2352.

[7]Raymer, D. P., Wilson, J., Perkins, H. D., Rizzi, A., Zhang, M., and Puentes, A. R., "Advanced Technology Subsonic Transport Study: N+3 Technologies and Design Concepts," NASA/TM-2011-217130, 2011.

[8]Beltramo, M. N., Trapp, D. L., Kimoto, B. W., and Marsh, D. P., "Parametric Study of Transport Aircraft Systems Cost and Weight," NASA CR-151970, 1977.

[9]Ardema, M. D., Chambers, M. C., Patron, A. P., Hahn, A. S., Miura, H., and Moore, M. D., "Analytical Fuselage and Wing Weight Estimation of Transport Aircraft," NASA/TM-110392, 1996.

[10]Cavagna, L., Ricci, S., and Riccobene, L., "Structural Sizing, Aeroelastic Analysis, and Optimization in Aircraft Conceptual Design," *Journal of Aircraft*, Vol. 48, No. 6, 2011, pp. 1840-1855.

[11]Chiozzotto, G. P., "Wing weight estimation in conceptual design: a method for strut-braced wings considering static aeroelastic effects," *CEAS Aeronautical Journal*, Vol. 7, 2016, pp. 499-519.

[12]Dorbath, F., *A Flexible Wing Modeling and Physical Mass Estimation System for Early Aircraft Design Stages*, Ph.D. Thesis, TU Hamburg-Harburg, 2014.

[13]Kelm, R., Läpple, M., and Grabietz, M., "Wing primary structure weight estimation of transport aircrafts in the pre-development phase," Society of Allied Weight Engineers Paper 2283, May 1995.

[14]Torenbeek, E., "Development and Application of a Comprehensive, Design-sensitive Weight Prediction Method for Wing Structures of Transport Category Aircraft," TU Delft LR-693, TU Delft, 1992.

[15]York, P., and Labell, R. W., "Aircraft Wing Weight Build-up Methodology with Modifications for Materials and Construction Techniques," NASA CR-166173, 1980.

[16]Scott, P. W., and Nguyen, D., "The Initial Weight Estimate," Society of Allied Weight Engineers Paper 2327, Jun. 1996.

[17]Böhnke, D., *A Multi-Fidelity Workflow to Derive Physics-Based Conceptual Design Methods*, Ph.D. Thesis, TU Hamburg-Harburg, DLR-Forschungsbericht 2015-09, 2015.

[18]Bradley, K. R., "A Sizing Methodology for the Conceptual Design of Blended-Wing-Body Transports," NASA/CR-2004-213016, 2004.

[19]Jemitola, P. O., Monterzino, G., and Fielding, J., "Wing mass estimation algorithm for medium range box wing aircraft," *The Aeronautical Journal*, Vol. 117, No. 1189, 2013, pp. 329-340.

[20]Skillen, M. D., and Crossley, W. A., "Developing Response Surface Based Wing Weight Equations for Conceptual Morphing Aircraft Sizing," *AIAA/ASME/ASCE/AHS/ASC Structures, Structural Dynamics & Materials Conference*, AIAA Paper 2005-1960, Apr. 2005.

[21]Redeker, G., and Wichmann, G., "Forward Sweep – A Favorable Concept for a Laminar Flow Wing," *Journal of Aircraft*, Vol. 28, No. 2, 1991, pp. 97-103.

[22]Risse, K., Schäfer, K., Schültke, F., and Stumpf, E., "Central Reference Aircraft data System (CeRAS) for research community," *CEAS Aeronautical Journal*, Vol. 7, 2016, pp. 121-133.

[23]Loftin, L. K., "Subsonic Aircraft: Evolution and the Matching of Size to Performance," NASA RP-1060, 1980.

[24]Shevell, R. S., *Fundamentals of Flight*, Prentice-Hall Inc., Englewood Cliffs, New Jersey, 1983.

[25]Ekvall, J. C., and Griffin, C. F., "Design Allowables for T300/5208 Graphite/Epoxy Composite Materials," *Journal of Aircraft*, Vol. 19, No. 8, 1982, pp. 661-667.

[26]MSC.Software Corporation, Nastran 2010, MSC.Software Corporation, Santa Ana, CA, 2010.

[27]Mason, W., "Analytic Models for Technology Integration in Aircraft Design," *AIAA/AHS/ASEE Aircraft Design, Systems and Operations Conference*, AIAA Paper 90-3262, Sept. 1990.

[28]Keane, A. J., and Nair, P. B., *Computational Approaches for Aerospace Design: The Pursuit of Excellence*, John Wiley & Sons Ltd, Chichester, 2005.

[29]Klimmek, T., *Statische aeroelastische Anforderungen beim multidisziplinären Strukturentwurf von Transportflugzeugflügeln*, Ph.D. Thesis, TU Braunschweig, DLR-Forschungsbericht 2016-34, 2016.

[30]Bradley, M. K., Droney, C. K., and Allen, T. J., "Subsonic Ultra Green Aircraft Research Phase II: Volume I - Truss Braced Wing Design Exploration," NASA CR-2015-218704/Volume I, 2015.